Supplemental Figure Legends

Supplemental Figure 1:
Extension of Figure 2A with additional examples of axonal enrichment of transfected versions of Tau^{D2}
Different isoforms of Tau^{D2} were cotransfected with tdTomato for 6 days into primary neurons (7DIV) derived from TauKO as indicated. tdTomato was used as a volume and morphology marker. Columns 1,2, are the same as Fig. 2A and shown for comparison.
Transfected Tau was stained with an antibody against human Tau (CP27). A biased distribution (axonal enrichment) appears for Tau in most cases, in contrast to the unbiased distribution of tdTomato. Green color in merged images indicates enrichment of Tau. Arrowheads indicate the axon, arrows indicate dendrites.
Transfected isoforms are indicated, mutations are on the basis of 2N4R-Tau. Note that axonal enrichment is strongest for 0NxR isoforms (columns 1,2,10), and least pronounced for 2N4R-Tau (columns 5,6). Other Tau isoforms show intermediate to strong axonal enrichment (columns 3,4,7,8,9). Note that shown mutations of Tau are sorted stronger in the axon than unmodified 2N4R-Tau (columns 11,12,13).

Supplemental Figure 2:
Extension of Figure 2B with additional examples of axonal enrichment of transfected versions of Tau^{D2}
Different isoforms of Tau^{D2} were cotransfected with tdTomato for 6 days into primary neurons (7DIV). Wildtype neurons expressing endogenous Tau in addition to transfected exogenous Tau^{D2} (stained with CP27, green color). Exogenous and endogenous Tau is stained with a panTau antibody (K9JA), dendrites are stained with an antibody against MAP2. Colums 1,2,4,5,6 are the same as Fig. 2B and shown for comparison.
A biased distribution (axonal enrichment) appears for Tau in most cases, in contrast to the unbiased distribution of tdTomato (red color). Green color in merged images indicates enrichment of Tau. Arrowheads indicate the axon, arrows indicate dendrites.
Columns 1, 2: 0N4R-Tau is enriched in the axon. As a result, axonal Tau concentration is higher than in neighboring untransfected axons where only endogenous Tau is present, but can barely be detected in dendrites with a panTau antibody. Col 2, bottom shows magnified images from boxed areas, axon is indicated by arrowheads.
Columns 3: 1N4R is apparent in the axon.
Columns 4, 5: 2N4R-Tau is very little present in the axon, enrichment (compared to the dendrite) is not apparent (note similar color of red-green merge of axon compared to dendrite).
Columns 6,7,8: 2N4R-Tau pseudophosphorylated at the KXGS-motifs (KXGS-motifs phosphorylated to KXGE, column 6), or carrying the mutation deltaK2802P (column 7) or A152T (columns 8), show strong axonal enrichment compared to unmutated 2N4R-Tau.

Supplemental Figure 3:
Structural components of the AIS contribute to the tightness of the retrograde and anterograde Tau Diffusion Barrier.
(A,B) Major structural components of the AIS contribute to the retrograde TDB integrity. Primary cortical neurons were cotransfected with 2N4R-Tau^{PSCFP2} and shRNA (either control or shRNA against an AIS constituent, as indicated).
(A) Representative pictures 1h after photoconversion of 2N4R-Tau in the axon (indicated by red rectangles). While in control condition 2N4R-Tau does not reach the cell body (A1, red circle), in cells that have been transfected with shRNA for knocking down EB1 Tau appears in the cell body (A2, red circle).
(B) Diagram shows quantification of cell body intensities in the photoconverted channel 1h after photoconversion. Knockdown of several proteins known to be major structural components of

the AIS (e.g. Ankyrin G, NaV, βIV-spectrin, EB1, EB3, NrCAM) but not of an unrelated control (Spastin) leads to retrograde propagation of Tau from the axon into the soma.
(C) Major structural components of the AIS contribute to the anterograde TDB integrity. Primary cortical neurons were cotransfected with 2N4R-Tau^{D2} and shRNA (either control or shRNA against an AIS constituent, as indicated) plus a volume marker (tdTomato).
Cotransfection of 2N4R-Tau^{D2} and tdTomato reveals little propagation of Tau into the axon in control conditions (C1), but enhanced axonal enrichment in case of knockdown of EB1 (C2), arrows indicate the axon.
(D) Quantification of axonal presence (relative to the cell body) of 2N4R-Tau^{D2} and MAP2 invasion into the proximal axon. Note that in most knockdowns MAP2 levels in the proximal axon increase, but only in some cases (AnkG, βIV-spectrin, EB1) Tau presence increases.

Supplemental Figure 4:
Knockdown of AIS structural components does not result in endogenous missorting of Tau into the soma.
Primary cortical neurons DIV9-11 where transfected with shRNA constructs as indicated plus tdTomato as a transfection marker.
(A) Overview images of transfected cells (red color) and stainings against Tau (antibodies K9JA and DA9, green color) and against the AIS structural components (in the examples shown 2nd antibody control (A1), EB1 (antibody 5/EB1; A2) and NrCAM (rabbit polyclonal antibody; A3). Boxed areas are magnified in B, D, E as indicated.
(B) Magnified images of control cells and knockdowns of EB1 from (A1, A2). There is no accumulation of Tau in the cell body (cell body circumference is indicated by dotted line).
(C) Quantification of Tau in the cell body shows that knockdown of structural components of the AIS (as indicated) does not lead to missorting of Tau.
(D,E) Example of successful knockdown of EB1 (D2, compare with control cell of D1) and NrCam (E2, compare with control cell of E1).

Supplemental Figure 5:
GSK3β transfection results in missorting of endogenous Tau
(A) Primary rat hippocampal neurons 18DIV were transfected with GSK3β fused to RFP via adenovirus mediated gene transfer for 3d. Asterisks indicate transfected cells. Tau was stained with an antibody against total Tau (K9JA), Tau phosphorylated at the KXGS-motifs was stained using 12E8 antibody.
(A1) Left panels: GSK3β transfected cells show missorting of Tau and enhanced phosphorylation at KXGS-motifs (arrows), while neighboring cells do not show presence of Tau in dendrites, and only background phosphorylation at the KXGS-motifs.
Right panels: Treatment of a culture transfected with GSK3β results in missorting of Tau also in cells not transfected with GSK3β (arrowheads), but with thinner dendrites than the cells expressing GSK3β (arrows). Treatment with Aβ does not increase missorting of Tau in GSK3β transfected cells.
(A2) Quantification of A1 reveals significant differences between cells treated with Aβ and GSK3β.
(B) Primary neurons aged 20DIV were treated with Aβ and phosphorylation of GSK3β was examined with an antibody recognizing GSK3β when phosphorylated at S9.
(B1) Quantification of pGSK3β (indicative of inactivated GSK3β) show a steam rise after 5-30min of Aβ-treatment, and a return to baseline within 3 hours.
(B2) Representative images of a control cell (upper panel) and a cell treated with Aβ for 15min (lower panel). The latter shows increased levels of GSK3β phosphorylation at S9 both in the cell body (asterisk) and the dendrites (arrows).

Supplemental Figure 6:
Wildtype and constitutively active, but not inactive, GSK3β results in missorting of Tau and increased density of dendritic microtubules.
GSK3β was transfected as wildtype (left panels), active form (S9A mutant, middle panels) and inactive form (S9E mutant, right panels) for 5d in rat cortical primary neurons 10DIV, cells were then fixed and stained as indicated.
(A) Wildtype and active GSK3β, but not inactive GSK3β, induce increase of microtubule density in dendrites. Cells were fixed, extracted and stained for microtubules. Arrows indicate dendrites (A1), which are magnified in A2.

Supplemental Figure 7:
Volume normalization of measurements shown in Figure 4 and pictograms demonstrate that microtubule PTM are different in the cell body, AIS and axon.
Thin lines show measurements, thick lines show moving averages of measurements.
(A-C) Volume normalization of measurements shown in Figure 4. Values of A-C are calculated by dividing values presented in Figure 4 by values of tdTomato shown in (D) and rescaled for illustration.
(A) Tyrosination of microtubules rapidly decreases from the cell body through the AIS to attain very low levels in the axon.
(B) Acetylation of microtubules is very low at the beginning of the AIS, intermediate in the cell body and the distal AIS, and high in the axon.
(C) Polyglutamylation is very low in the cell body and the beginning of the AIS but rapidly increases within the AIS and attains high levels in the axon.
(D) Not normalized intensity measurements of the volume marker for tdTomato show the differences of volumes throughout the different compartments, assuming unbiased distribution of tdTomato.

Supplemental Figure 8:
Aβ is targeted to the AIS and reduces AIS levels of F-actin and AnkyrinG
Rat primary cortical neurons 21 DIV were exposed for 1h to 1µM Aβ oligomers and stained as indicated.
(A) Primary rat neurons were exposed to Aβ for 1h, fixed and stained for Aβ with a monoclonal antibody which does not recognize APP (DE2), for the AIS with an antibody against NrCAM, and MAP2 to identify dendrites. Boxed areas in the left panel are shown magnified on the right. Dendritic spines and dendrites show strongest targeting by Aβ, AIS shows little targeting by Aβ, while axons are largely devoid of Aβ targeting. Lower right panel shows quantification of immunofluorescence intensities in the different compartments as indicated by letters a (dendrites), b (AIS) and c (axon).
(B) Neurons stained for AnkyrinG and MAP2 to identify and measure fluorescence intensities within the AIS.
(C) Measurements along the AIS indicated a localized decrease of f-actin within the central part of the AIS (C1), i.e. within the first 5-10µm, and an overall decrease of AnkyrinG (C2) already after 1h of treatment. This indicates that although the AIS might overall be slightly affected, the F-actin decrease is predominant in the central part. (C3) shows statistical significance of the AnkyrinG measurements in C2 when comparing the Area under the curve (AUC, 0-15µm) after background subtraction (1000 units).

Supplemental Figure 9:
Tau^{D2} shows no signs of aberrant degradation in N2a cells and primary neurons
(A,B) Tau^{D2} is not degraded in neuroblastoma cells after photoconversion. N2a neuroblastoma cells were transfected with Tau^{D2} and subsequently cultured for two days. Cells in the whole field were then photoconverted and the intensity of photoconverted Tau^{D2} was followed for 20 hours.
(A) Images show examples of photoconverted cells before (upper left) and after photoconversion as indicated. Note that the upper and lower cell have divided at 12h. Cells show membrane associated fluorescence indicative of the membrane association of Tau.
(B) Quantification of the field of (A) reveals that there is no decrease after 1h of photoconversion, and only a trend to decreased intensities after 5-20h possibly caused by internal Tau relocalization (membrane trapping away from the confocal volume) or bleaching.
(C1,2) Tau^{D2} does not get degraded in primary neurons. Primary cortical neurons 7-8DIV were transfected with Tau^{D2} for 3d and then treated with cycloheximide (CHX) to block protein synthesis for up to 24h. Cells were lysed and immunoblotted with an antibody against total Tau (K9JA). There is no apparent decrease in protein levels of Tau^{D2}, in contrast to endogenous Tau.

Supplemental Tables

Supplemental Table 1: Summary of the phenotypes in primary forebrain neurons induced by low expression of Tau^{D2} isoforms.

Tau clone nomenclature	Isoform of Tau	mutation	Axonal enrichment of hTau	Spine number*	Spine length*	Spine maturity* /**	Dendrite length
hTau40	2N4R	none	+	+	o	+++	+++
hTau34	1N4R	”	++	+	+	++	n.d.
hTau24	0N4R	”	+++	+	+	+	+
hTau39	2N3R	”	++	++	++	++	+++
hTau37	1N3R	”	+	+	+	+	n.d.
hTau23	0N3R	”	+++	++	+++	o	+
	2N4R	4KxGA	+	+	o	+	+
	”	4KXGE	+++	+	+	+	+
	”	A152T	++	+++	++	++	++
	”	ΔK280	++	+	+	+	++
	”	ΔK280-PP	++	++	++	++	+++

Legend: o: not apparent; +: apparent; ++ strong; +++ very strong; n.d. not determined
*positive change in spine parameters relative to control conditions
**spine head apparent (as indicator of maturity)

Supplemental Table 2: List of antibodies used in the study, for details see methods.

antibody (clone/name)	dilution	species	company/provider
Aβ (DE2)	1:50-1:300	mouse	Millipore
acetylated Tubulin (611B1)	1:500-1:1000	mouse	Sigma
Ankyrin-G (N106/36)	1:200-1:300	mouse	NeuroMab
CP27	1:100	mouse	Davies
EB1 (5/EB1)	1:100	mouse	BD Laboratories
EB3	1:200	rabbit	Thermo Scientific
F-Actin (CF350 Phalloidin)	1:50-1:100		Biotium
F-Actin (CF405 Phalloidin)	1:50		Biotium
GSK3β pS9	1:50-1:100	rabbit	Cell signaling
MAP2	1:5000-1:10000	chicken	abcam
NrCam	1:200-1:1000	rabbit	abcam
Polyglutamyl. Tubulin (B3)	1:500-1:1000	mouse	Sigma
p-cofilin (Ser3) (4317)	1:200	rabbit	James Bamburg
pTau (12E8)	1:200-1:500	mouse	Elan
Tau (DA9)	1:40-1:500	mouse	Davies
Tau (K9JA)	1:100-1:500	rabbit	Dako
Thyrosin. Tubulin (YL1/2)	1:300-1:1000	rat	serotec
Tubulin (DM1α)	1:300	mouse	Sigma
2N Tau (71C11)	1:500	mouse	BioLegend

Figure S1

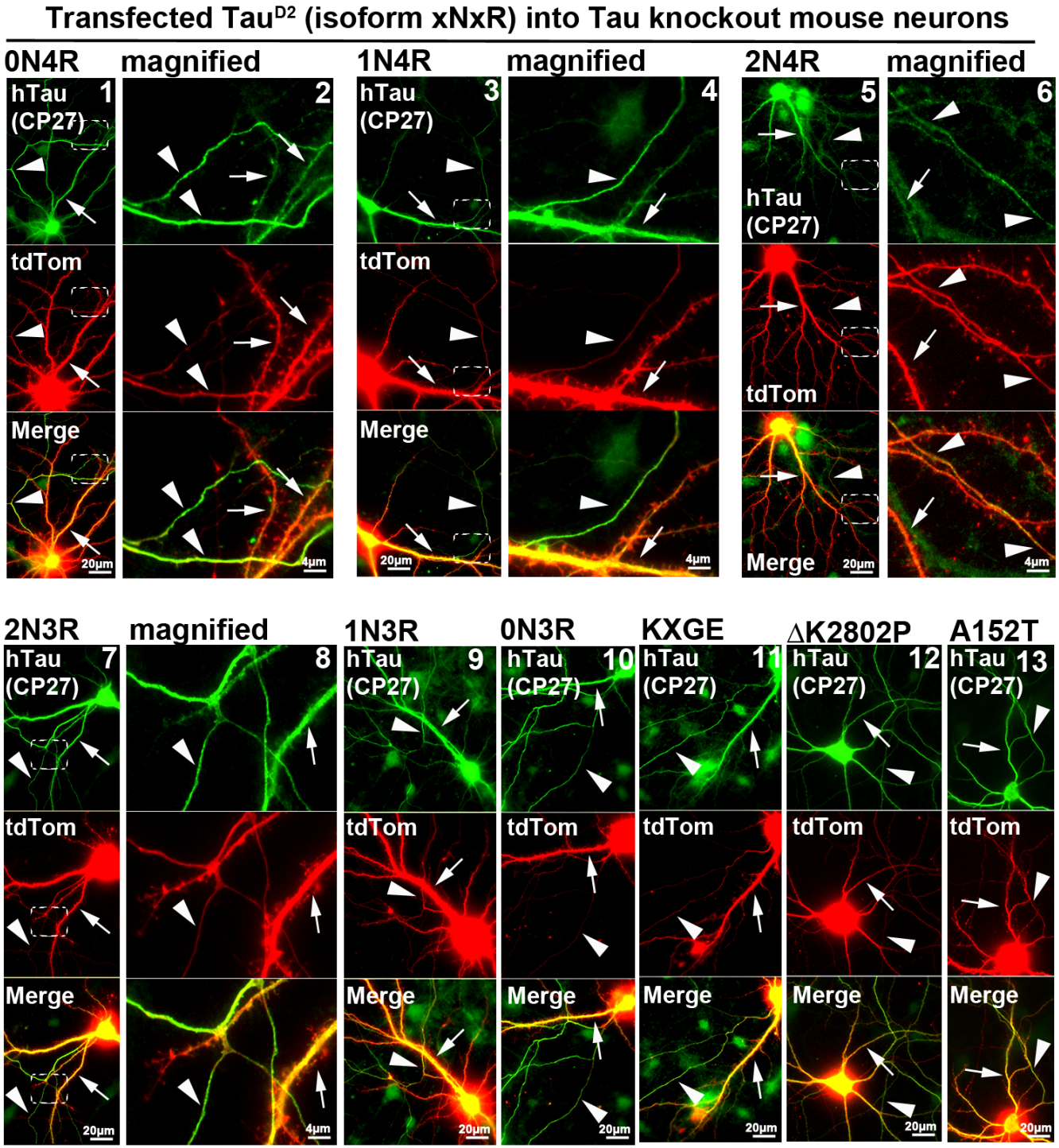
Transfected Tau^{D2} (isoform xNxR) into Tau knockout mouse neurons
0N4R
magnified
1N4R
magnified
2N4R
magnified
2N3R
magnified
1N3R
0N3R
KXGE
ΔK2802P
A152T
hTau (CP27)
tdTom
Merge
1
2
3
4
5
6
7
8
9
10
11
12
13
20μm
4μm

Figure S2

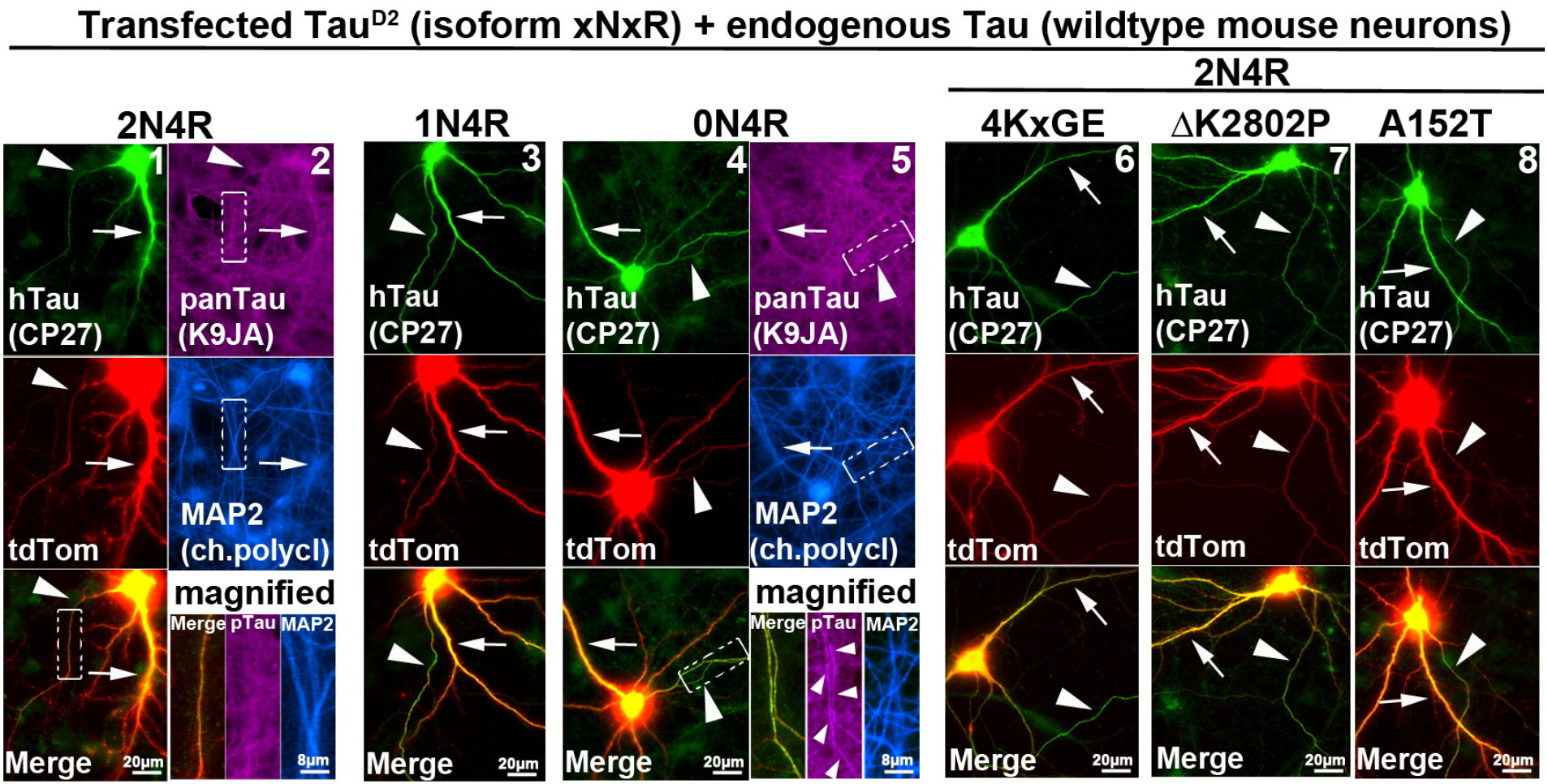
Transfected Tau^{D2} (isoform xNxR) + endogenous Tau (wildtype mouse neurons)
2N4R
1N4R
0N4R
2N4R
4KxGE
ΔK2802P
A152T
1
2
3
4
5
6
7
8
hTau (CP27)
panTau (K9JA)
MAP2 (ch.polycl)
tdTom
magnified
Merge
pTau
MAP2
20μm
8μm

Figure S3

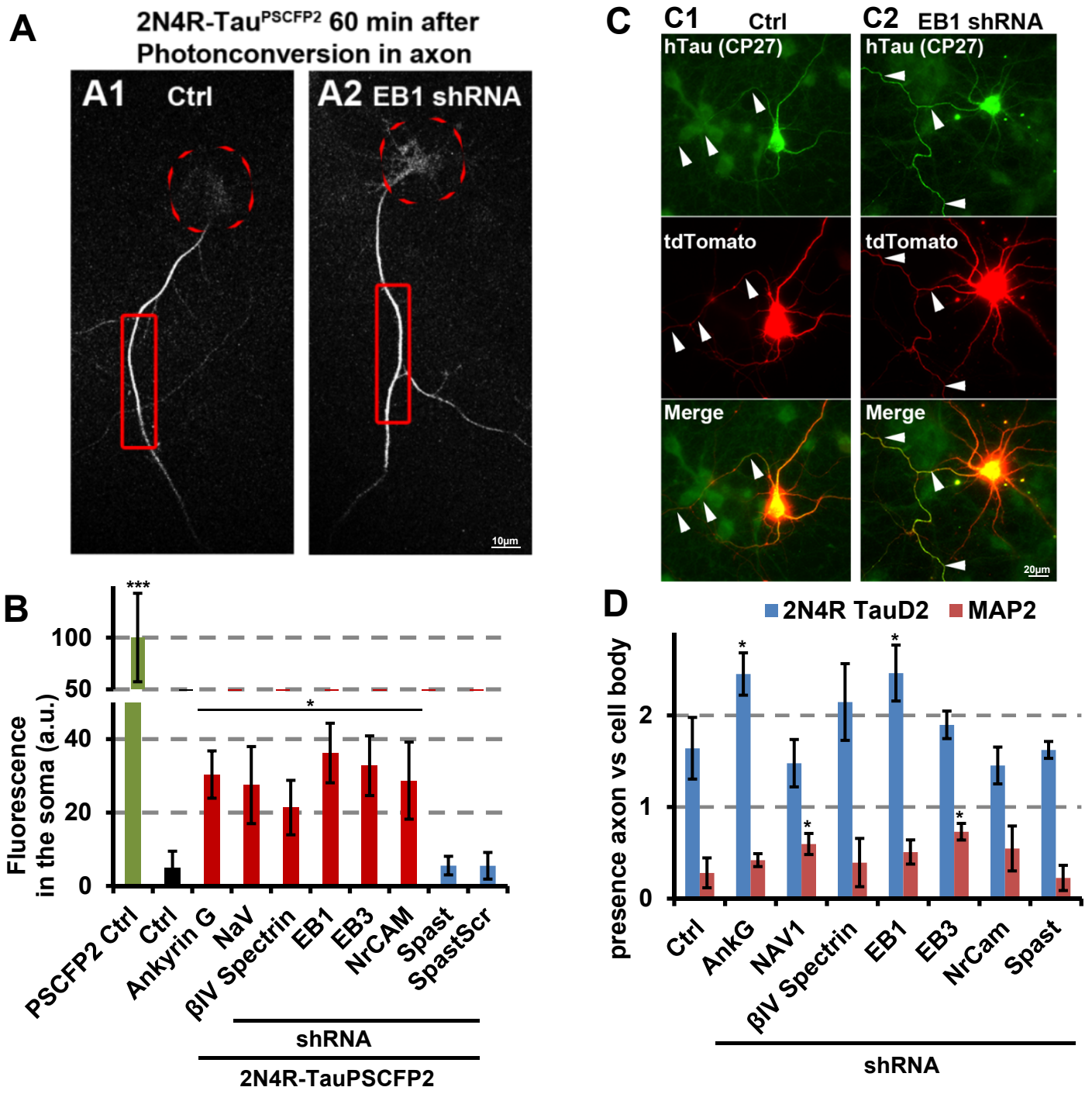
A
2N4R-Tau^PSCFP2 60 min after Photonconversion in axon
A1 Ctrl
A2 EB1 shRNA
10µm
B
Fluorescence in the soma (a.u.)
100
50
40
20
0
***
*
PSCFP2 Ctrl
Ctrl
Ankyrin G
NaV
βIV Spectrin
EB1
EB3
NrCAM
Spast
SpastScr
shRNA
2N4R-TauPSCFP2
C
C1 Ctrl
C2 EB1 shRNA
hTau (CP27)
tdTomato
Merge
20µm
D
2N4R TauD2
MAP2
presence axon vs cell body
2
1
0
Ctrl
AnkG
NAV1
βIV Spectrin
EB1
EB3
NrCam
Spast
shRNA

Figure S4

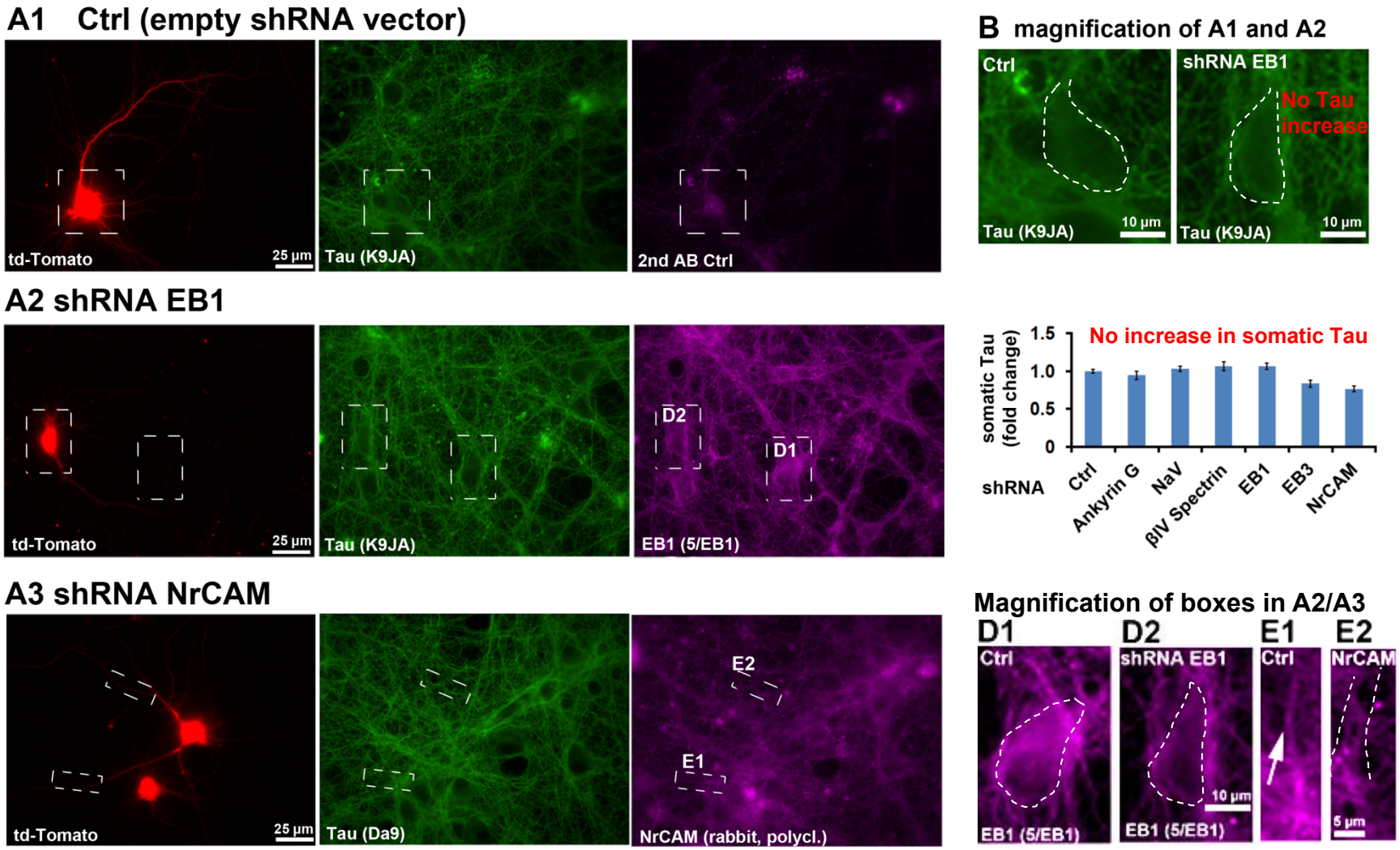
A1 Ctrl (empty shRNA vector)
td-Tomato
25 µm
Tau (K9JA)
2nd AB Ctrl
A2 shRNA EB1
td-Tomato
25 µm
Tau (K9JA)
D2
D1
EB1 (5/EB1)
A3 shRNA NrCAM
td-Tomato
25 µm
Tau (Da9)
E2
E1
NrCAM (rabbit, polycl.)
B magnification of A1 and A2
Ctrl
Tau (K9JA)
10 µm
shRNA EB1
No Tau increase
Tau (K9JA)
10 µm
No increase in somatic Tau
somatic Tau (fold change)
1.5
1.0
0.5
0
shRNA
Ctrl
Ankyrin G
NaV
βIV Spectrin
EB1
EB3
NrCAM
Magnification of boxes in A2/A3
D1
Ctrl
EB1 (5/EB1)
D2
shRNA EB1
10 µm
EB1 (5/EB1)
E1
Ctrl
E2
NrCAM
5 µm

Figure S5

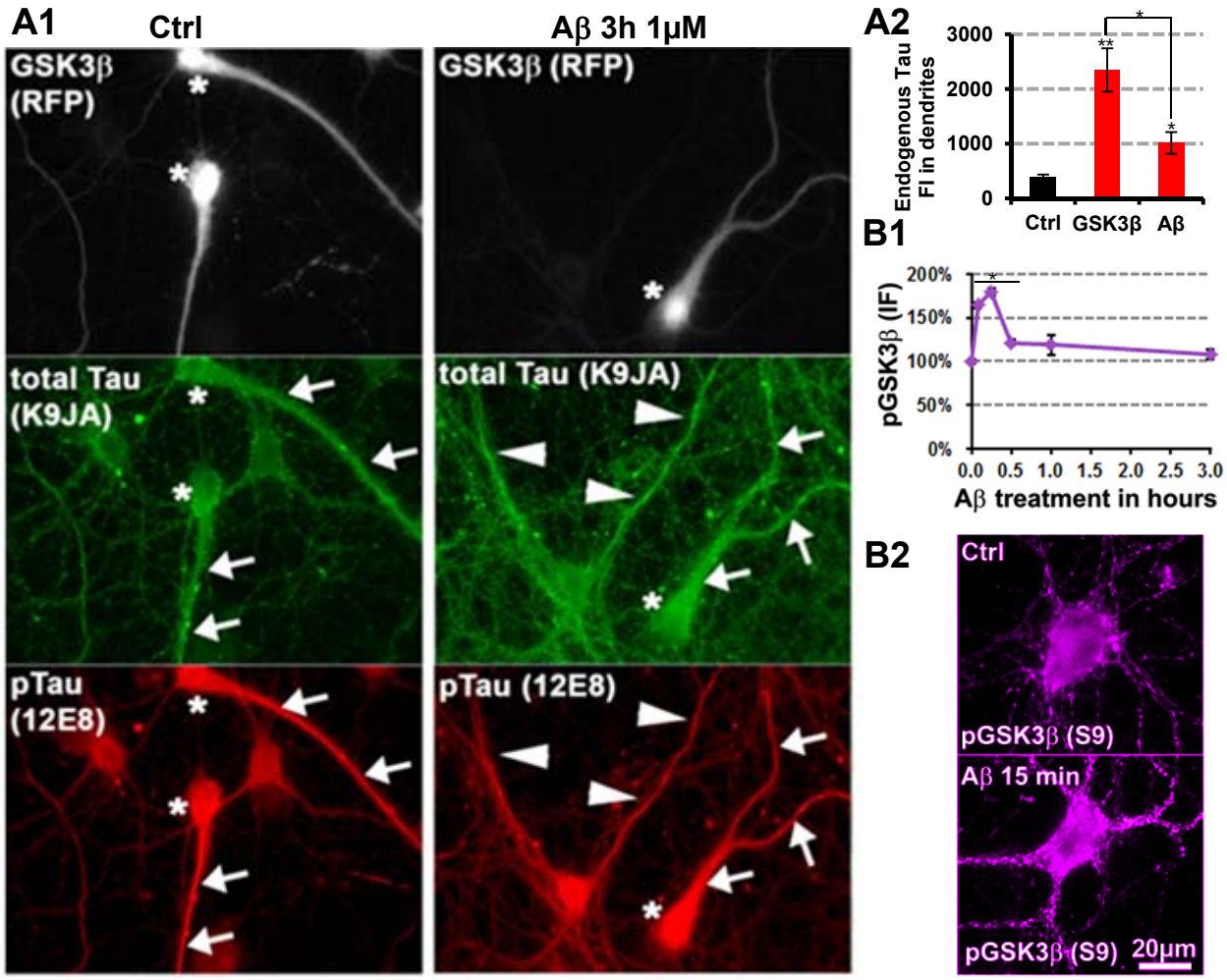
A1
Ctrl
Aβ 3h 1μM
GSK3β (RFP)
total Tau (K9JA)
pTau (12E8)
A2
Endogenous Tau FI in dendrites
3000
2000
1000
0
Ctrl
GSK3β
Aβ
B1
pGSK3β (IF)
200%
150%
100%
50%
0%
0.0 0.5 1.0 1.5 2.0 2.5 3.0
Aβ treatment in hours
B2
Ctrl
pGSK3β (S9)
Aβ 15 min
pGSK3β (S9)
20μm

Figure S6

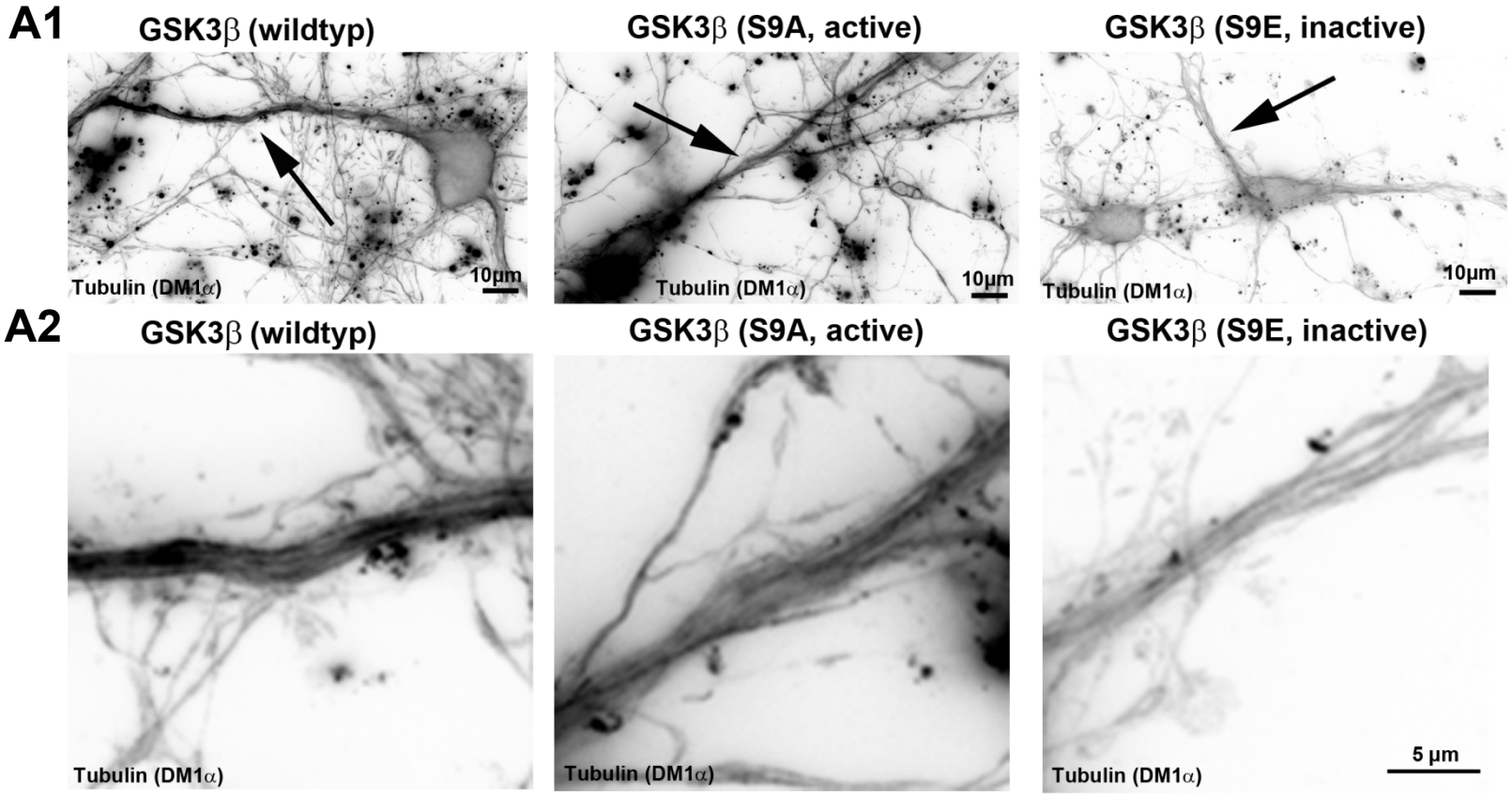
A1
GSK3β (wildtyp)
GSK3β (S9A, active)
GSK3β (S9E, inactive)
Tubulin (DM1α)
10µm
Tubulin (DM1α)
10µm
Tubulin (DM1α)
10µm
A2
GSK3β (wildtyp)
GSK3β (S9A, active)
GSK3β (S9E, inactive)
Tubulin (DM1α)
Tubulin (DM1α)
Tubulin (DM1α)
5 µm

Figure S7

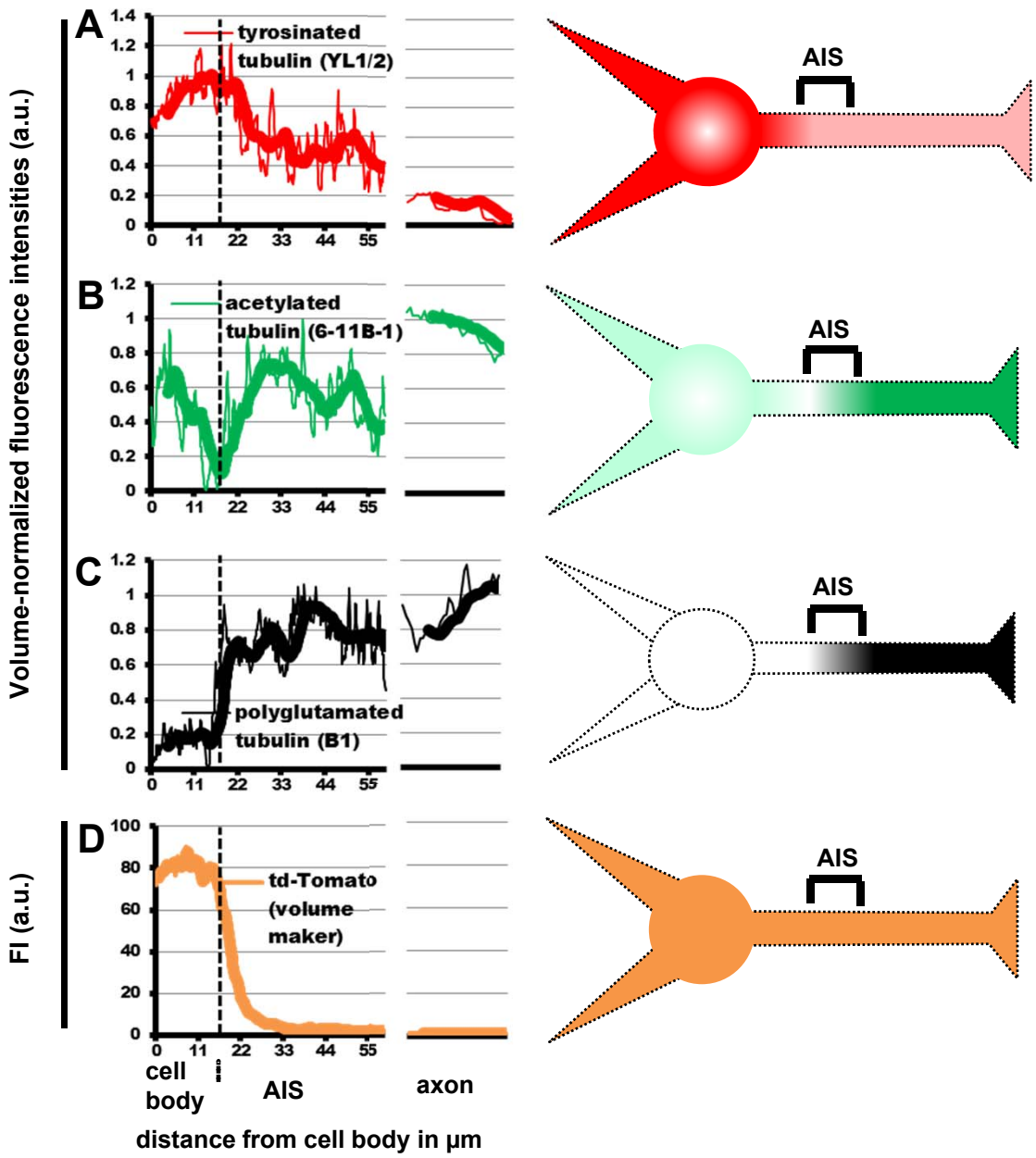
A
tyrosinated
tubulin (YL1/2)
B
acetylated
tubulin (6-11B-1)
C
polyglutamated
tubulin (B1)
D
td-Tomato
(volume
maker)
AIS
AIS
AIS
AIS
Volume-normalized fluorescence intensities (a.u.)
FI (a.u.)
cell
body
AIS
axon
distance from cell body in µm

Figure S8

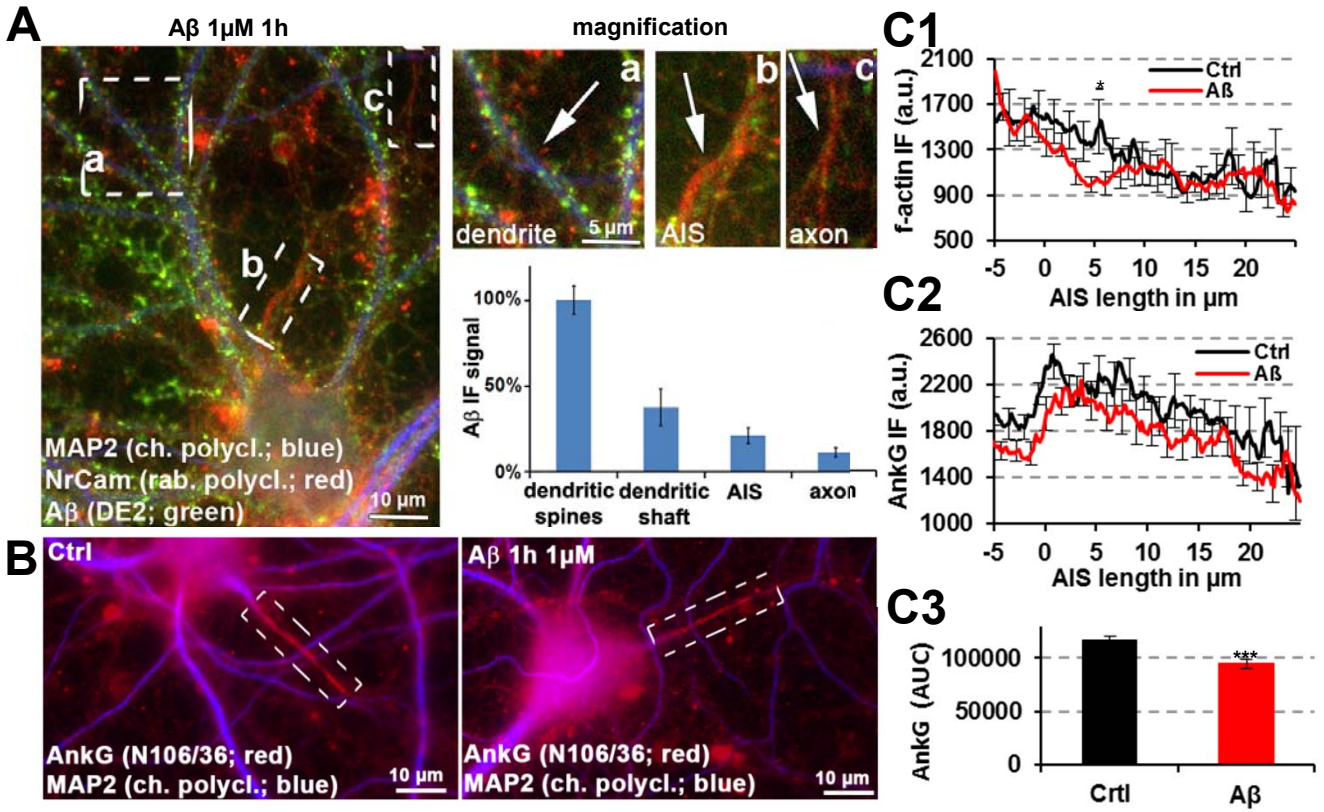
A
Aβ 1μM 1h
magnification
a
b
c
MAP2 (ch. polycl.; blue)
NrCam (rab. polycl.; red)
Aβ (DE2; green)
10 μm
dendrite
5 μm
AIS
axon
Aβ IF signal
100%
50%
0%
dendritic spines
dendritic shaft
AIS
axon
B
Ctrl
Aβ 1h 1μM
AnkG (N106/36; red)
MAP2 (ch. polycl.; blue)
10 μm
C1
f-actin IF (a.u.)
2100
1700
1300
900
500
Ctrl
Aß
*
-5 0 5 10 15 20
AIS length in μm
C2
AnkG IF (a.u.)
2600
2200
1800
1400
1000
Ctrl
Aß
-5 0 5 10 15 20
AIS length in μm
C3
AnkG (AUC)
100000
50000
0
***
Crtl
Aβ

Figure S9

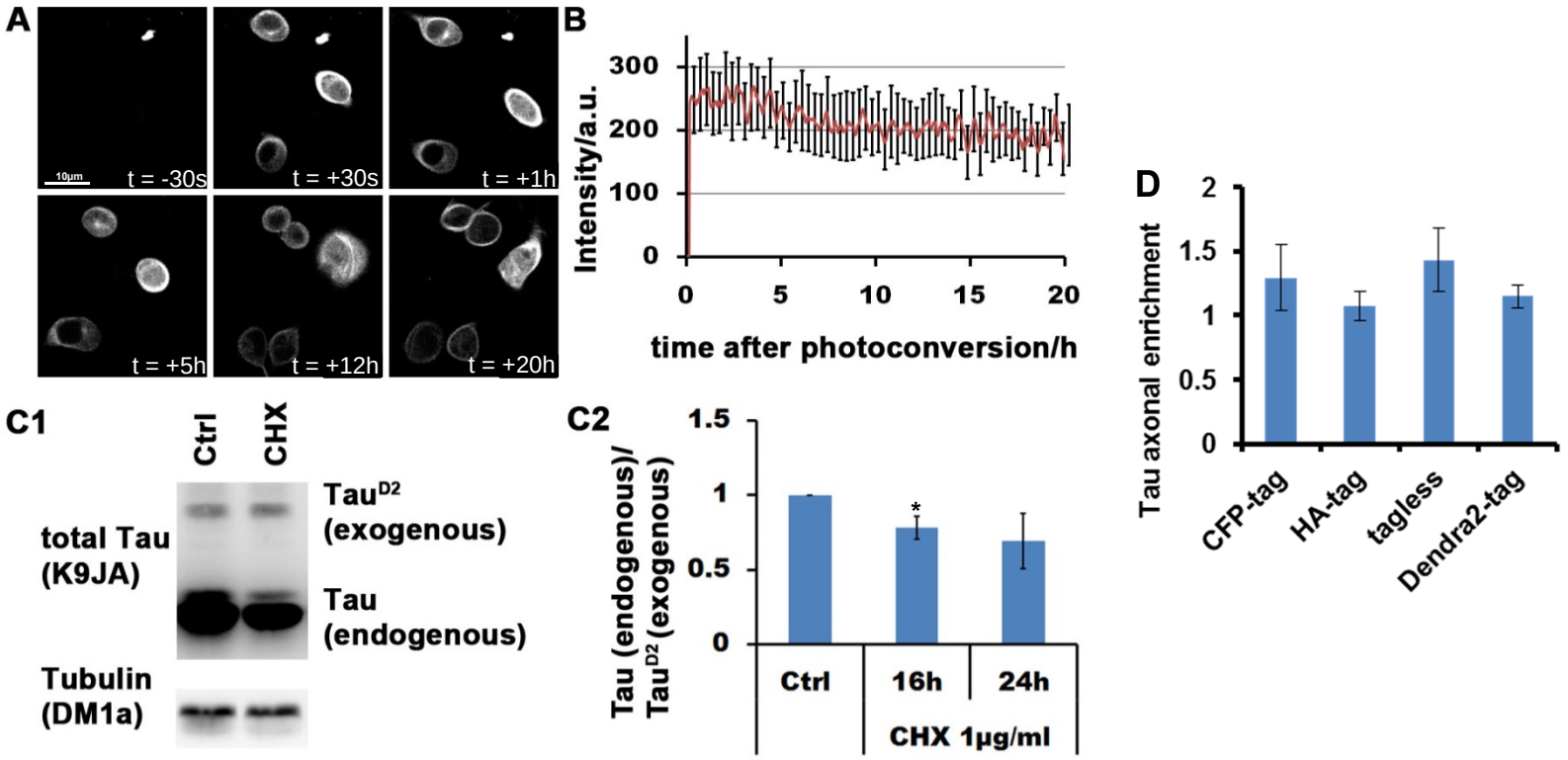
A
10µm
t = -30s
t = +30s
t = +1h
t = +5h
t = +12h
t = +20h
B
Intensity/a.u.
300
200
100
0
0
5
10
15
20
time after photoconversion/h
C1
Ctrl
CHX
total Tau
(K9JA)
Tau^{D2}
(exogenous)
Tau
(endogenous)
Tubulin
(DM1a)
C2
Tau (endogenous)/
Tau^{D2}(exogenous)
1.5
1
0.5
0
*
Ctrl
16h
24h
CHX 1µg/ml
D
Tau axonal enrichment
2
1.5
1
0.5
0
CFP-tag
HA-tag
tagless
Dendra2-tag